Academia
Green Energy

10.20935/AcadEnergy8409

Research Article

Magnesium chloride saltwater solutions as phase change material for sub-zero thermal energy storage

Thandiwe Bongani Radebe[1], Lucas Sekele[2], Asasei Unarine Casey Ndanduleni[1], Lehlogonolo Rudolf Kanyane[1], Zhongjie Huan[1,*], Washington Mhike[1,*], Innocentia Boingontlo Setlhabi[1], James Molelekoa Mosesane[1]

[1] Faculty of Engineering and Built Environment, Tshwane University of Technology, Pretoria, South Africa
[2] School of Science, University of South Africa, Pretoria, South Africa
* Correspondence: huanz@tut.ac.za (Z.H.); mhikew@tut.ac.za (W.M.)

Received: 23 March 2026 | **Accepted:** 25 June 2026 | **Published:** 9 July 2026

Abstract

Introduction: Efficient sub-zero latent heat thermal energy storage (LHTES) is critical for decarbonizing refrigerated transport. While aqueous magnesium chloride ($MgCl_2$) is a highly promising inorganic phase change material (PCM), its industrial deployment is severely limited by phase transition anomalies, severe supercooling, and aggressive corrosivity.

Materials and methods: This study investigates the thermodynamic and electrochemical behaviour of $MgCl_2$ solutions (14–25 wt.%) to resolve existing literature discrepancies regarding hypereutectic phase boundaries and to establish optimal containment parameters.

Results: Differential scanning calorimetry (DSC) and bulk-scale cooling protocols revealed that rapid thermal gradients kinetically suppress primary hydrate precipitation in 25 wt.% solutions, inducing a metastable state that solidifies *en masse* near −34 °C rather than the predicted equilibrium liquidus. Furthermore, macro-scale evaluations (500 g) demonstrated significant thermal lag compared to micro-scale baselines, driven by the low intrinsic thermal conductivity of the crystalline matrix. To resolve the containment bottleneck, potentiodynamic polarisation and 480 h ASTM G31 immersion tests evaluated aluminium, copper, and 316L stainless steel. Aluminium exhibited rapid passive layer breakdown and severe chloride-induced pitting, evidenced by $Al(OH)_3$ precipitation. Conversely, 316L stainless steel demonstrated superior localised corrosion resistance and a stable passivation layer ($i_{corr} \approx 1.5$ μA cm^{-2}).

Conclusions: Ultimately, a 21 wt.% eutectic $MgCl_2$ solution paired with 316L stainless steel provides the optimum thermodynamic and structural configuration for next-generation sub-zero heat exchangers.

Keywords: magnesium chloride; phase change materials; sub-zero thermal energy storage; eutectic solutions; corrosion resistance; latent heat

1. Introduction

The increasing demand for refrigeration and cold-chain logistics has intensified global energy consumption and associated greenhouse gas emissions. Refrigerated storage and transportation systems are essential for

maintaining food quality, pharmaceutical integrity, and thermal stability throughout the supply chain; however, their continuous operation requires substantial energy input. Consequently, improving the energy efficiency of refrigeration systems has become an important research priority within the broader context of sustainable energy management and decarbonisation strategies [1, 2].

Cold thermal energy storage (CTES) technologies have attracted considerable attention because of their ability to decouple cooling generation from cooling demand, thereby reducing peak electrical loads and improving refrigeration system performance. Among the available thermal energy storage technologies, latent heat thermal energy storage (LHTES) systems employing phase change materials (PCMs) are particularly attractive because they can store and release large amounts of thermal energy at nearly constant temperatures during phase transitions [1, 3]. Recent studies have reported that PCM-integrated refrigeration systems can improve temperature regulation, reduce compressor cycling, enhance system efficiency, and increase operational flexibility in cold-storage applications [2].

Phase change materials are generally classified as organic, inorganic, and eutectic materials. Among these categories, inorganic salt hydrates have received significant research attention because of their high latent heat storage capacity, relatively high thermal conductivity, low cost, and favourable volumetric energy storage density [4]. Despite these advantages, inorganic salt hydrates continue to exhibit several limitations, including supercooling, phase segregation, thermal instability, low cycling reliability, and corrosion-related challenges, which restrict their large-scale implementation in thermal energy storage systems [4].

Magnesium chloride hydrate ($MgCl_2 \cdot 6H_2O$) has emerged as a promising inorganic phase change material for low-temperature and sub-zero thermal energy storage applications. Magnesium chloride-based systems possess favourable thermophysical properties, including high energy storage density and phase transition temperatures suitable for refrigerated storage and cold-chain applications [5, 6]. According to Yang et al. [6], magnesium chloride hydrate phase change materials demonstrate significant potential for cold-storage engineering owing to their high latent heat storage capacity and ability to maintain stable low-temperature thermal environments. Furthermore, recent investigations have shown that variations in hydration state, water content, and concentration significantly influence the phase transition characteristics and thermal storage performance of magnesium chloride hydrate systems [6].

To overcome the inherent limitations of salt hydrate phase change materials, numerous enhancement strategies have been investigated. These include nano-additive incorporation, porous support structures, encapsulation techniques, composite PCM development, and thermal conductivity enhancement approaches [4, 7]. Wu et al. [8] developed a $MgCl_2$–H_2O eutectic nanofluid containing multi-walled carbon nanotubes and reported reduced supercooling behaviour together with improved thermal conductivity. Similarly, Jiang et al. [5] highlighted the importance of thermophysical optimisation in magnesium chloride-based thermal energy storage systems, while recent reviews have emphasised the continuing need to improve the thermal reliability and heat transfer performance of inorganic salt hydrate PCMs [4].

Although substantial progress has been achieved in enhancing magnesium chloride-based phase change materials, a significant proportion of the available literature focuses on modified systems containing nanoparticles, composite matrices, or conductivity-enhancing additives. Comparatively fewer studies have systematically investigated the concentration-dependent thermal behaviour of unmodified $MgCl_2$–H_2O solutions across a concentration range relevant to sub-zero thermal energy storage applications. Furthermore, most thermophysical investigations have been conducted using small-scale differential scanning calorimetry techniques, while

limited information is available regarding the influence of sample mass on solidification and melting behaviour under larger-scale conditions [9].

In addition to thermodynamic performance, corrosion remains a critical challenge for chloride-based thermal energy storage systems. Chloride-containing media are known to promote localised corrosion and passive-film degradation in metallic materials, potentially affecting the long-term reliability of thermal energy storage containers, heat exchangers, and refrigeration components. Consequently, the practical implementation of magnesium chloride-based phase change materials requires simultaneous evaluation of both thermal performance and material compatibility. However, studies integrating thermophysical characterisation and corrosion assessment within a unified experimental framework remain limited.

Therefore, the present study investigates the thermal and corrosion characteristics of $MgCl_2$–H_2O solutions with concentrations ranging from 14 wt.% to 25 wt.% for sub-zero latent heat thermal energy storage applications. Differential scanning calorimetry was employed to determine phase transition temperatures and latent heat capacities, while macro-scale melting and solidification experiments were conducted to evaluate the influence of concentration and thermal mass on phase change behaviour. In addition, immersion testing and potentiodynamic polarisation analyses were performed to assess the corrosion behaviour of aluminium, copper, and stainless steel exposed to $MgCl_2$ solutions. The study provides a comprehensive assessment of both thermophysical performance and material compatibility, contributing to the development of magnesium chloride-based cold thermal energy storage systems for refrigeration and cold-chain applications.

While the literature often cites the equilibrium eutectic point of aqueous $MgCl_2$ at approximately 21 wt.% and −33.6 °C, previous bulk-scale investigations by the authors [10] revealed significant thermodynamic anomalies, particularly at higher concentrations (e.g., 25 wt.%), where empirical phase behaviours drastically deviated from theoretical liquidus boundaries (typically reported near −19 °C). To resolve this discrepancy and establish accurate baseline parameters for cold-chain heat exchangers, this study systematically investigates the $MgCl_2$ phase envelope across the critical 14–25 wt.% range to quantify the effects of metastable supercooling, mass-dependent thermal lag, and localised containment corrosion.

2. Materials and methods

Industrial grade magnesium chloride hexahydrate ($MgCl_2 \cdot 6H_2O$; Chem Lab Supplies, Johannesburg, South Africa) with a minimum purity of 98.5% was used in this study. The material had a molecular weight of 203.30 g/mol, a relative density of 1570 g/cm^3, and a melting point of 116.7 °C. **Table 1** presents the maximum impurity limits of the $MgCl_2 \cdot 6H_2O$ used. Deionised water (Chemical Engineering Department, Tshwane University of Technology, Pretoria, South Africa) was used for all solution preparations to minimise the influence of impurities.

Table 1. Magnesium chloride ratio.

$MgCl_2$ (wt.%)	14	15	16	17	18	19	20	21	22	23	24	25
$MgCl_2$ (g)	7	7.5	8	8.5	9	9.5	10	10.5	11	11.5	12	12.5

2.1. Thermal analysis

2.1.1. Preparation of $MgCl_2$ saltwater samples

$MgCl_2$ saltwater solutions were prepared with concentrations ranging from 14 wt.% to 25 wt.%. The mixtures were prepared in 0.5 L containers using an analytical balance with an accuracy of ±0.00001 g. These ratios are displayed in **Table 1**.

2.1.2. Solidification phase change temperature determination

Type K thermocouples with a maximum accuracy of (were ±2.5 °C or ±0.75 °C) inserted into the solution and connected to a GL820 Graphtec data logger (Graphtec, Shanghai, China) to monitor the temperature change. Samples were inserted into a laboratory BDF-86V160 ultra-freezer (Biobase, Shandong, China) already stabilised at −80 °C. Cooling was achieved through natural convection in refrigerated air; no cryogenic liquid immersion was used.

2.1.3. Melting phase change temperature determination

The frozen samples were removed from the ultra-freezer and allowed to melt at ambient room temperature (20 ± 1 °C). Temperature changes were continuously recorded using the same data recording system as in the solidification phase.

2.1.4. Effects of sample mass

To investigate the effect of sample mass on phase change behaviour, experiments were conducted with 50 g and 500 g samples. For 500 g samples, Pt100 probes spanned the container depth to account for thermal gradients. Type K thermocouples monitored temperature change at single-point locations in smaller samples. The experimental bifurcation into 50 g and 500 g configurations is methodologically necessary to evaluate macro-scale thermal lag. As established by recent composite thermal characterizations [11], expanding the physical volume and subsequent thermal mass of a salt hydrate matrix alters internal heat transfer distribution, changing the supercooling profiles and phase-segregation behaviour that are typically observed on a micro-scale during controlled differential scanning calorimetry (DSC) runs [12].

2.2. Differential scanning calorimetry (DSC)

Latent heat measurements were performed using a PerkinElmer DSC 6000 (PerkinElmer South Africa (Pty) Ltd., Midrand, South Africa). Samples of 25 ± 0.1 mg were sealed in aluminium pans. The following thermal cycle was used:

- Equilibration at 25 °C for 1 min;
- Cooling to −80 °C at a rate of 1 °C/min;
- Isothermal hold at −80 °C for 1 min;
- Heating to 0 °C at a rate of 1 °C/min.

Measurements were made for $MgCl_2$ concentrations of 17%, 21%, and 25%.

2.3. Corrosion tests

2.3.1. Sample preparation

Corrosion tests were performed on three common metals used in refrigeration systems:

- Aluminium 5754 (supplied by Non-Ferrous Metal Works (SA) (Pty) Ltd., Pretoria, South Africa);
- Copper tube material (supplied by TecsaReco, Pretoria, South Africa);
- 316L stainless steel.

Metal samples were cut from larger plates into 5 × 2 mm, cleaned with acetone to remove surface oils, and weighed using an analytical balance (±0.00001 g precision).

2.3.2. Immersion tests

Fourteen samples of each metal were immersed in 25% $MgCl_2$ solutions for 4 weeks. The 25 wt.% concentration was utilised for immersion testing to simulate the most aggressive, highest-chloride environment the containment vessels might experience. Visual inspections were carried out at 48 h intervals, noting changes in colour, precipitation, and mass loss. The corrosion rate of the metallic specimens was calculated following the ASTM G31 standard practice [13].

2.3.3. Potentiodynamic polarisation tests

The electrochemical corrosion behaviour was evaluated using a PGSTAT302N Autolab potentiostat (Metrohm AG, Sandton, South Africa) equipped with Nova software. A three-electrode cell with a metal sample was used as the working electrode, a platinum counter electrode, and a saturated calomel reference electrode. Polarisation curves were obtained by scanning from −150 mV to +150 mV versus open circuit potential at a scan rate of 0.5 mV/s.

3. Results

3.1. DSC results

The DSC thermograms for H_2O, 17% $MgCl_2$, 21% $MgCl_2$, and 25% $MgCl_2$ are shown in **Figure 1a–c** for PCM during the heating phase. From **Figure 1a**, the vertical line marks the analysed area and the Delta H represents the measured latent heat, H_2O started melting at 0 °C with a peak melting of 4.3 °C where the water crystal had fully melted. From **Figure 1b–d** the measured latent heat 17%, 21% and 25% $MgCl_2$ saltwater the latent heats were 24.6582 J/g, 171.3410 J/g, and 137.0490 J/g. The melting temperature of approximately −35 °C in the DSC thermograms corresponds to the melting temperature recorded in the PCM samples shown in **Figure 2**. The curves had a sharp heat flow curve before reaching −30 °C.

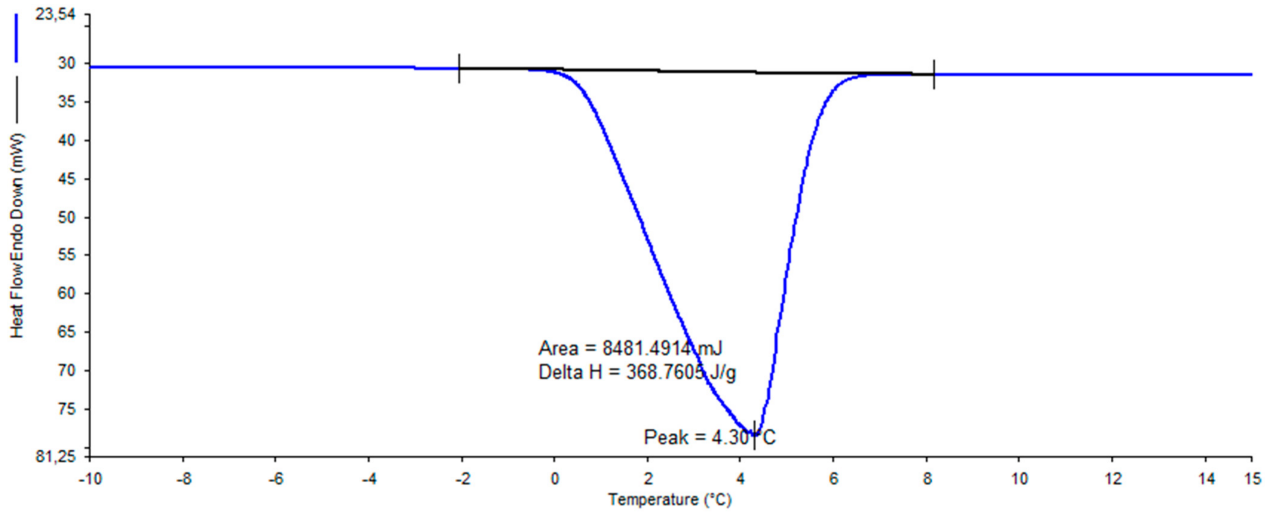

(**a**)

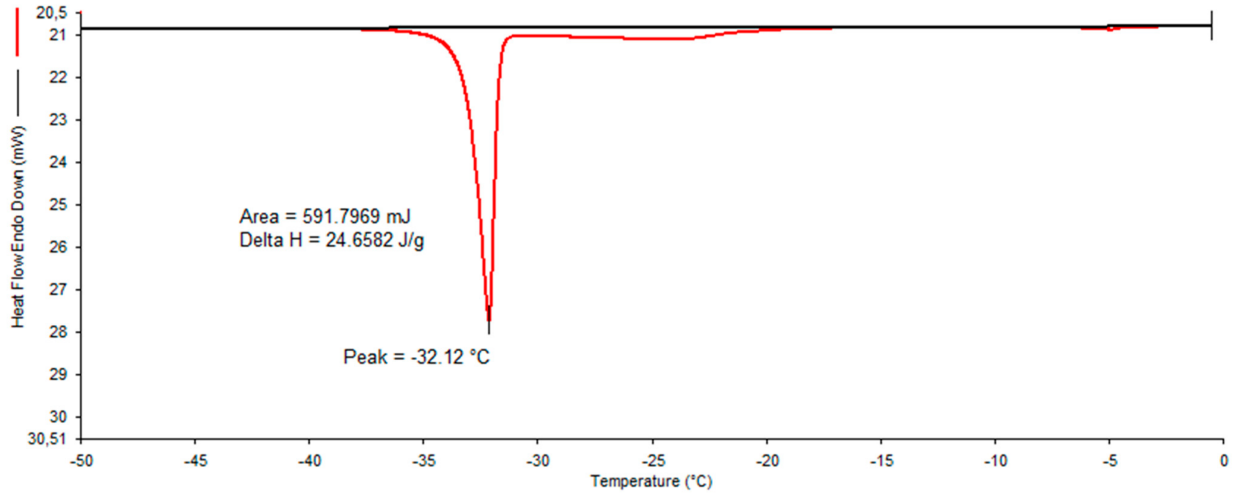

(**b**)

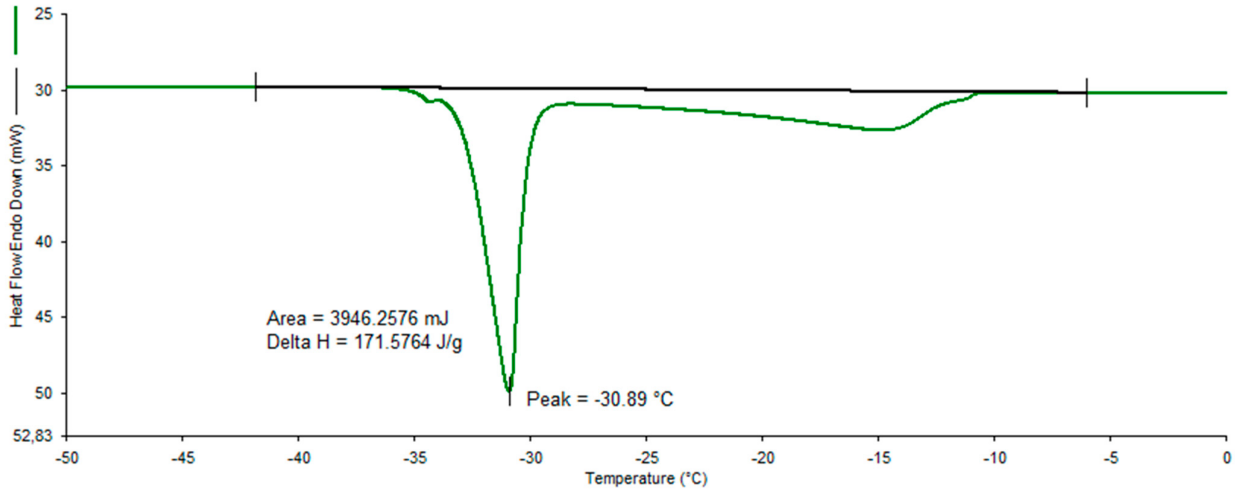

(**c**)

Figure 1. *Cont.*

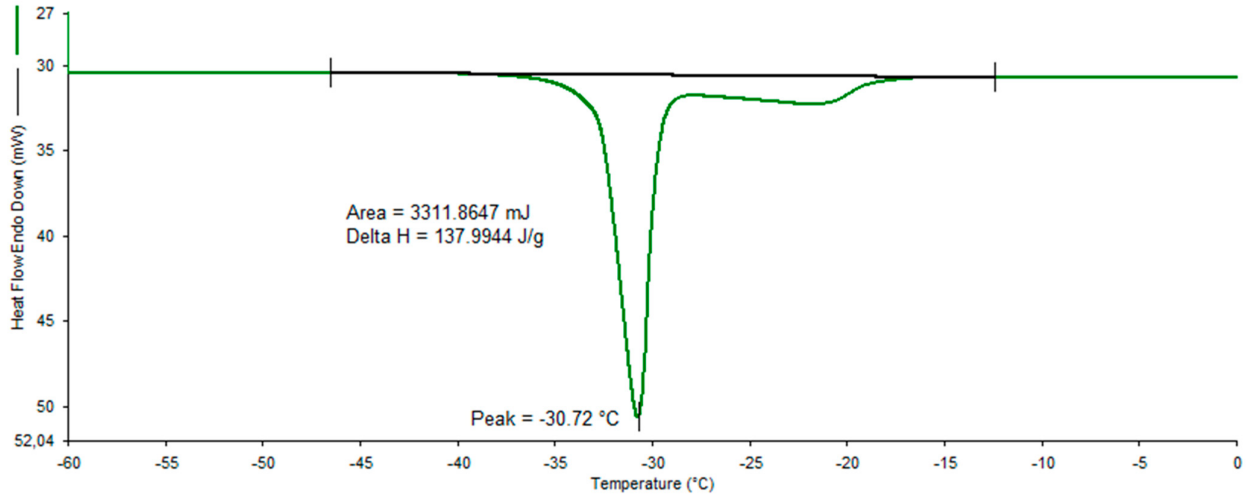

(**d**)

Figure 1. (**a**) H_2O Differential scanning calorimetry (DSC) thermogram; (**b**) 17% $MgCl_2$ DSC thermogram; (**c**) 21% $MgCl_2$ DSC thermogram; (**d**) 25% $MgCl_2$ DSC thermogram. Delta H represents the measured latent heat; the vertical line marks the analysed area.

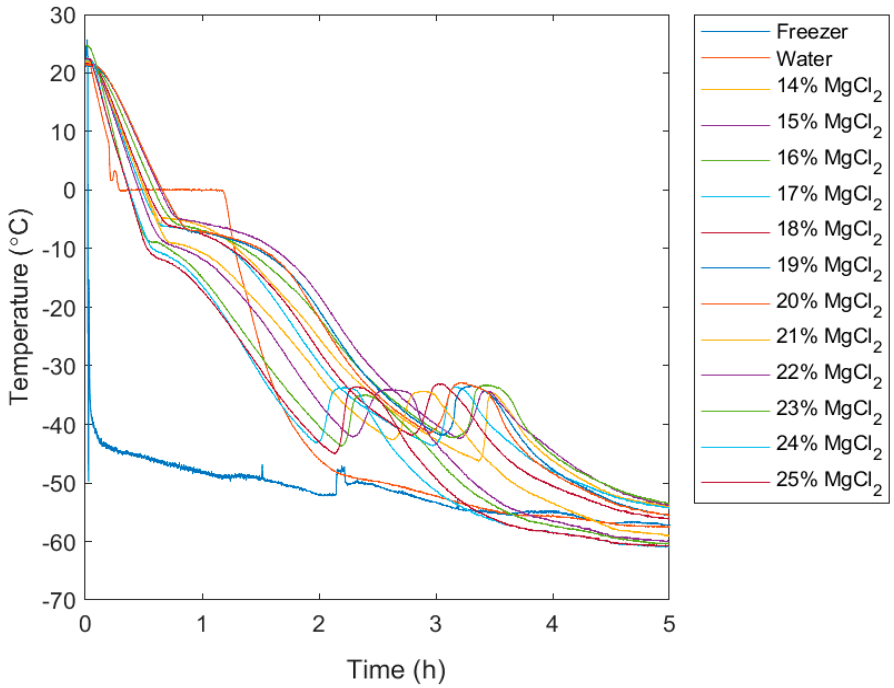

Figure 2. A total of 50 g of magnesium chloride solidification phase.

3.2. Solidification results

Figure 2 presents the solidification curves for $MgCl_2$ solutions with concentrations ranging from 14% to 25% by weight. All samples exhibited similar overall solidification patterns, characterised by three distinct stages: cooling, nucleation, and solidification. The cooling stage showed a near-linear temperature decrease until reaching a subcooling temperature of approximately −45 °C. Observed subcooling of −45 °C was consistent

across all concentrations. The nucleation stage was marked by a sharp increase in temperature, and all samples showed a supercooling degree of approximately 10 °C. The solidification stage showed more variation between concentrations. Higher $MgCl_2$ concentrations (20–25%) exhibited a steeper temperature increase and reached a higher plateau temperature compared to lower concentrations (14–19%). The presence of a temperature plateau around −10 °C for samples of lower concentration, lasting between 30 min and 1 h, was less pronounced or absent in samples with higher concentrations.

Figure 3 compares the solidification behaviour of 50 g and 500 g samples for selected concentrations of 25% $MgCl_2$. The larger mass samples showed overall patterns similar to their smaller counterparts, but with notable differences. In total, 500 g samples took significantly longer to fully solidify, and the 25% $MgCl_2$ solution took approximately 2 h longer in the 500 g sample compared to the 50 g sample. The temperature plateaus observed in the smaller samples were more pronounced and longer lasting in the 500 g samples, particularly for the lower concentrations. The initial cooling rate was slower in the 500 g samples, likely due to the larger thermal mass. Interestingly, the degree of supercooling (approximately 10 °C) remained consistent regardless of the sample mass.

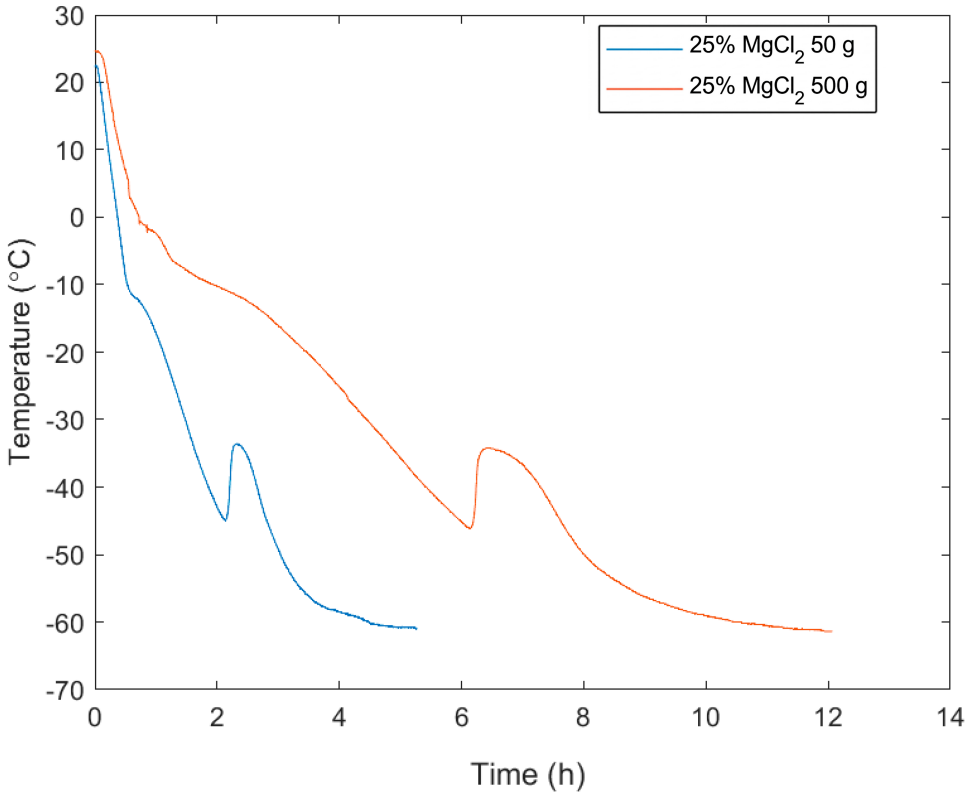

Figure 3. Comparison of 50 g and 500 g of magnesium chloride during the solidification phase.

3.3. Melting results

In **Figure 4**, the samples were exposed to ambient air that maintained a constant temperature of approximately 21 °C. The phase change temperature of the samples was −34 °C for higher concentration ratios and −32 °C for lower concentration ratios. **Figure 5** illustrates the comparison of 50 g and 500 g samples. Increasing the mass of the PCM increased the period of phase change temperature. Increasing the ratio from 17% to 25% also increased the phase change period. The 25% concentration ratio results in a phase change temperature of −34 °C.

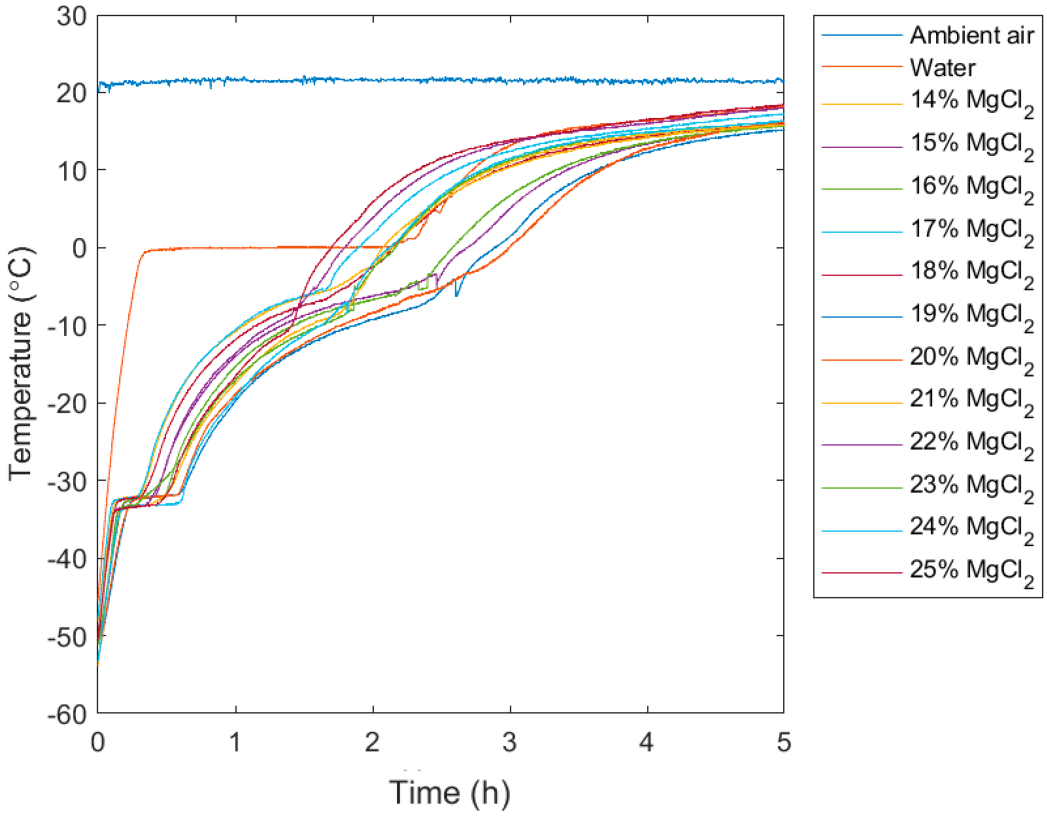

Figure 4. A total of 50 g of magnesium chloride solution during the melting phase.

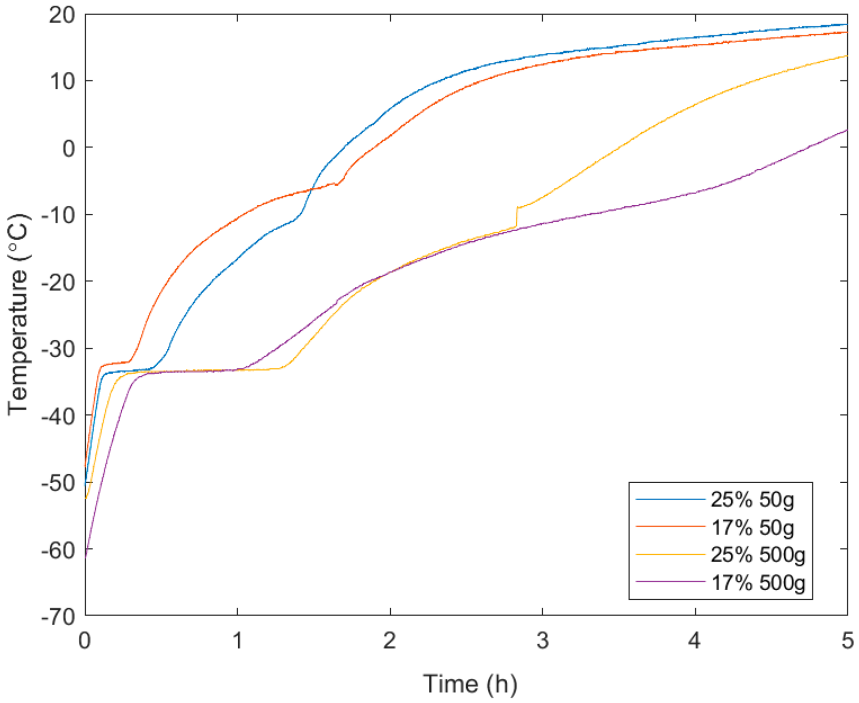

Figure 5. Comparison of 50 g and 500 g during the melting phase.

3.4. Corrosion results

The two subfigures, **Figure 6a,b**, present corrosion data for three different metals, aluminium, copper, and stainless steel, over a 30-day period. **Figure 6a** shows the mass loss (in g) over time, while **Figure 6b** displays the corrosion rate (in mg/cm^2/year) for the same materials and time frame. There is a clear correlation between the mass loss and corrosion rate patterns for each metal across both graphs. Aluminium exhibits the most volatile behaviour, with dramatic swings in both mass loss and corrosion rate, reaching the highest peaks and lowest troughs. Copper shows a more moderate pattern with gradual changes, while stainless steel demonstrates the least reactivity, staying closer to the zero line in both graphs. The peaks and valleys in mass loss for each metal correspond directly to the increases and decreases in the corrosion rate shown in **Figure 6a,b**, indicating a strong relationship between these two measures of corrosion. This correlation suggests that the mass loss data can be used to accurately predict corrosion rates, and vice versa, for these metals under the given conditions.

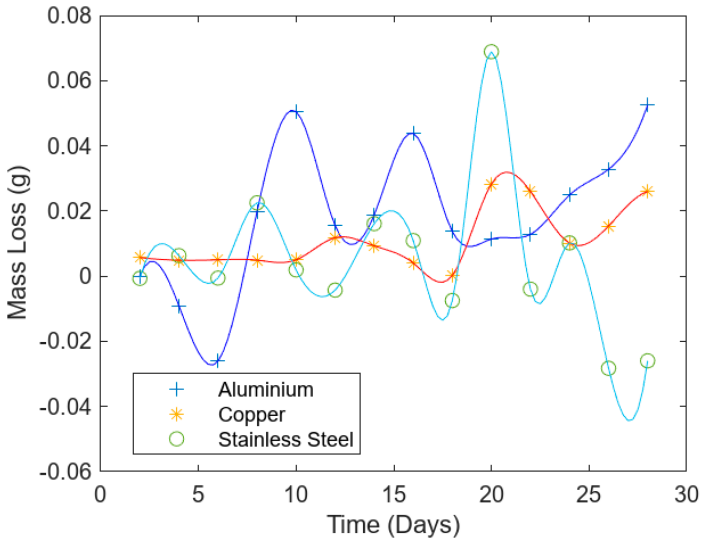

(**a**)

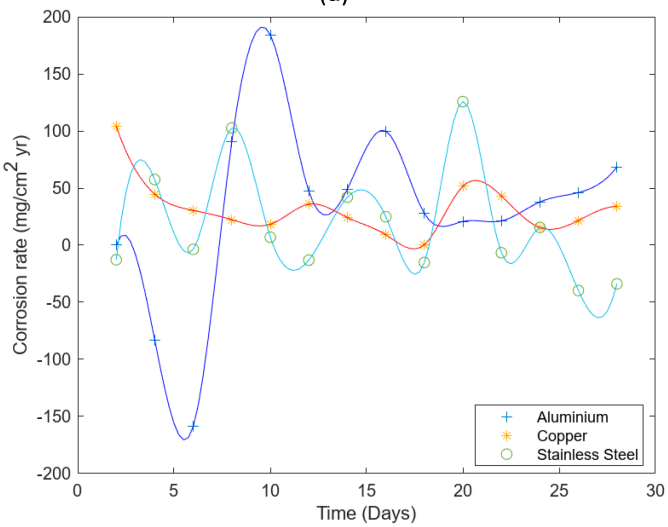

(**b**)

Figure 6. (**a**) Mass loss results of magnesium chloride saltwater; (**b**) corrosion rate results of magnesium chloride saltwater.

The industrial guide for weight loss from corrosion was used by Ferrer et al. [14]. Aluminium is not recommended for service longer than 1 year. Stainless steel showed a high corrosion rate of less than 100 mg/cm^2/year at the beginning, but was later reduced to a corrosion rate of less than 50 mg/cm^2/year. Stainless steel is also not recommended for service for more than a year; however, caution is recommended according to the specific application. For the copper metal used as an evaporator coil that maintained a corrosion rate of less than 50 mg/cm^2/year, Ferrer et al. [14] advises the designer to take precautions for the specific application.

Figure 7 presents the polarisation curves about the corrosion behaviour of these materials, including their corrosion potentials, passive regions, and breakdown potentials for three different materials: stainless steel (SS), aluminium (Al), and copper (Cu). Each material exhibits a distinct curve, illustrating their electrochemical behaviour. The SS curve shows typical passive behaviour with a wide passive region before a sharp increase in current at higher potentials. The Al curve demonstrates an active-passive transition with a clear passivation peak followed by a passive region. The Cu curve shows active dissolution without clear passivation. Al is known to have a tendency to form a passive oxide layer when exposed to an aggressive environment [15]. Although Al showed stable oxide behaviour, Al_2O_3 was prone to attack by Cl ions, which accelerated corrosion due to the current density of 0.0001 A/cm^2. However, Stainless steel exhibited a low corrosion current density (1.5×10^{-6} A/cm^2), consistent with Cr_2O_3 passive layer formation. However, Cl^- ions may still initiate localised breakdown of passivation under prolonged exposure [16].

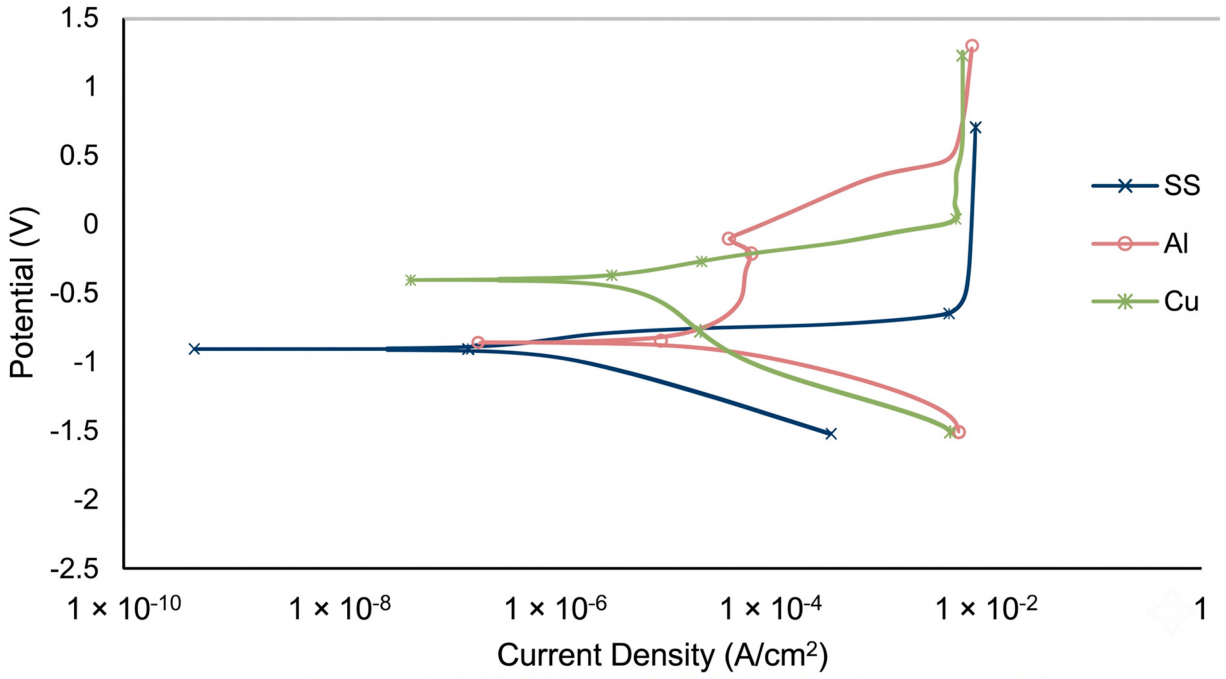

Figure 7. Potentiodynamic polarisation response of $MgCl_2$ solution at room temperature.

For aluminium, visual inspection of the immersion test electrolytes provided empirical validation of the potentiodynamic degradation mechanisms. The $MgCl_2$ solution containing aluminium developed a distinct milky-white suspension. This directly indicates the precipitation of aluminium hydroxide $Al(OH)_3$, a secondary byproduct formed when localised acidic pits rapidly dissolve the aluminium matrix into the bulk neutral electrolyte. Similarly, the $MgCl_2$ electrolyte containing copper coupons exhibited a distinct blue coloration after the immersion period, confirming the continuous anodic dissolution of cupric ions (Cu^{2+}) into the solution, correlating with its relatively

high measured corrosion current density (i_{corr}). The recorded initial pH data for $MgCl_2$ was of 8.24, which shifted during the tests.

4. Discussion

4.1. Influence of $MgCl_2$ concentration on thermophysical performance

As outlined in **Table 2**, standard thermodynamic literature predicts that a 25 wt.% $MgCl_2$ solution (hypereutectic) should initiate the precipitation of primary hydrates ($MgCl_2$ $8H_2O$) near −19.4 °C. However, our DSC and bulk physical experiments recorded a unified melting transition heavily depressed to −34 °C. This deviation from the literature values in **Table 2** is not an experimental error, but rather empirical evidence of severe kinetic suppression. The rapid thermal gradient applied during our cooling protocols bypassed the equilibrium precipitation of higher hydrates, forcing the metastable supersaturated 25 wt.% solution to solidify *en masse* near the eutectic temperature. This confirms that in practical, rapid-cooling refrigeration scenarios, $MgCl_2$ solutions may not follow the equilibrium pathways predicted by historical studies.

Table 2. Thermophysical properties of magnesium chloride.

Material	Saltwater (%)	Phase change temperature (°C)	Density (kg/m³)	Latent heat (kJ/kg)	Reference
Magnesium chloride saltwater $MgCl_2 \cdot 6H_2O$	17.1	−33.6	N/A	221.86	[17–19]
	21.01	−33.5			[20]
	25	−19.4		223.10	[17, 21]

The thermophysical properties of $MgCl_2$–H_2O solutions exhibited a strong dependence on salt concentration. Among the investigated concentrations, the 21 wt.% solution demonstrated the highest latent heat capacity (171.34 J g^{-1}), whereas the 17 wt.% and 25 wt.% solutions exhibited significantly lower latent heat values of 24.66 J g^{-1} and 137.05 J g^{-1}, respectively. This behaviour suggests the existence of an optimum concentration range within which the thermodynamic characteristics of the $MgCl_2$–H_2O system approach eutectic conditions.

The enhanced latent heat observed at 21 wt.% may be attributed to favourable hydrate formation and phase equilibrium conditions, resulting in a larger fraction of material participating in the phase transition process. Similar concentration-dependent behaviour has been reported for salt hydrate systems, where deviations from the eutectic composition result in the formation of secondary phases that reduce the effective latent heat storage capacity [5, 6]. The substantially lower latent heat recorded for the 17 wt.% solution indicates that a significant proportion of the water phase likely crystallised independently of the hydrate structure, thereby reducing the latent heat associated with the phase transformation. Conversely, the reduction in latent heat observed at 25 wt.% may be associated with excess salt content and changes in hydrate stability, which alter the thermodynamic equilibrium of the system.

The measured phase transition temperatures indicate that all investigated solutions are suitable for sub-zero thermal energy storage applications. The observed phase change temperatures are consistent with the requirements of frozen-food storage and refrigerated transport systems, where operating temperatures typically range between −18 °C and −35 °C. These findings support previous studies that identified magnesium chloride hydrate

systems as promising candidates for cold thermal energy storage owing to their favourable low-temperature phase transition characteristics and relatively high energy storage density [1, 6].

4.2. Supercooling behaviour and thermal reliability

Although favourable latent heat storage characteristics were observed, all $MgCl_2$ solutions exhibited significant supercooling during solidification. Nucleation occurred at approximately −45 °C, resulting in an average supercooling degree of approximately 10 °C relative to the melting temperature. The occurrence of supercooling is a well-documented limitation of inorganic salt hydrate phase change materials and represents one of the primary barriers to their practical implementation [2, 4, 6].

Supercooling occurs when the liquid phase remains metastable below its equilibrium freezing temperature due to the absence of suitable nucleation sites. Under these conditions, crystallisation is delayed until sufficient thermodynamic driving force is available to initiate nucleation. The relatively consistent supercooling behaviour observed across all investigated concentrations suggests that nucleation kinetics rather than concentration effects dominate the freezing process within the examined concentration range.

Similar observations have been reported by [3, 22], who investigated $MgCl_2$–H_2O eutectic systems and demonstrated that the incorporation of multi-walled carbon nanotubes reduced supercooling by promoting heterogeneous nucleation. Likewise, recent reviews on salt hydrate phase change materials have highlighted the use of nucleating agents, porous support matrices, and nano-enhanced additives as effective strategies for mitigating supercooling and improving thermal reliability [2].

Although this study did not focus on reducing supercooling, from an engineering perspective, supercooling has important implications for thermal energy storage system performance. Excessive supercooling delays latent heat release during discharge, potentially reducing the effectiveness of the PCM under practical refrigeration conditions. Consequently, although the investigated $MgCl_2$ solutions demonstrate favourable thermal storage characteristics, future system development should incorporate strategies to suppress nucleation delay and improve thermal response reliability.

4.3. Scale effects: comparison between DSC and macro-scale thermal behaviour

One of the most significant findings of this study is the observed difference between micro-scale thermal characterisation and macro-scale phase change behaviour. Differential scanning calorimetry remains the most widely used technique for evaluating PCM thermophysical properties; however, the present results demonstrate that DSC measurements alone are insufficient for predicting large-scale system performance.

The macro-scale freezing and melting experiments revealed substantially longer phase transition durations compared with those implied by DSC measurements. Increasing sample mass resulted in extended freezing and melting times owing to larger thermal gradients and increased internal heat transfer resistance within the PCM volume. As the volume scales up, the low intrinsic thermal conductivity of the newly formed solid $MgCl_2$ hydrate acts as an insulating barrier. This traps the core heat, causing the massive thermal lag and prolonging the temperature plateaus. While latent heat values and phase transition temperatures obtained from DSC provide valuable information regarding intrinsic material properties, they do not fully capture the heat transfer limitations that emerge at larger scales.

This finding is particularly relevant for practical thermal energy storage systems, where PCM volumes are several orders of magnitude larger than those typically analysed using DSC. Similar scale-dependent behaviour has been reported in recent investigations of cold thermal energy storage systems, where increasing PCM volume altered phase transition kinetics and thermal response characteristics [6, 9]. Consequently, the combination of DSC and macro-scale experimentation employed in the present study provides a more realistic assessment of PCM performance under conditions representative of practical deployment.

The results further demonstrate that thermal mass plays a critical role in determining charging and discharging characteristics. Therefore, the design of cold thermal energy storage systems should account for both thermodynamic properties and heat transfer limitations to ensure accurate performance prediction.

4.4. Corrosion behaviour and material compatibility

In addition to thermal performance, material compatibility represents a critical consideration for the practical implementation of chloride-based phase change materials. The corrosion investigations revealed notable differences in the behaviour of aluminium, copper, and stainless steel when exposed to $MgCl_2$ solutions.

The relatively poor performance of aluminium can be attributed to chloride-induced breakdown of the protective aluminium oxide film. Chloride ions are known to penetrate passive oxide layers and initiate localised pitting corrosion, resulting in accelerated material degradation [15]. Similar behaviour has been widely reported for aluminium alloys exposed to chloride-containing environments.

Copper exhibited intermediate corrosion resistance, demonstrating greater stability than aluminium but remaining susceptible to electrochemical degradation in chloride-rich solutions. Although copper is frequently used in heat exchanger applications because of its high thermal conductivity, prolonged exposure to chloride-containing PCMs may compromise long-term durability.

Among the investigated materials, stainless steel exhibited the most favourable corrosion behaviour. The superior performance of stainless steel is attributed to the formation of a stable chromium-rich passive layer that provides enhanced resistance against chloride attack. Similar findings have been reported for thermal energy storage systems employing salt hydrate phase change materials, where stainless steel consistently demonstrated superior corrosion resistance compared with aluminium and copper [14, 15]. Stainless steel is superior for *uniform* corrosion resistance, but susceptible to *pitting* in high-chloride environments over long-term cycles. *Copper and aluminium* are rejected not just because of mass loss, but because of the specific chemistry: the blue/white byproducts noted in the inspection.

The corrosion results indicate that material selection plays a crucial role in determining system reliability. For practical implementation of $MgCl_2$-based thermal energy storage systems, stainless steel appears to be the most suitable containment material among those investigated.

4.5. Applicability of $MgCl_2$–H_2O solutions for sub-zero thermal energy storage

The suitability of a phase change material for refrigerated transport and cold storage applications depends on a combination of thermal performance, phase transition temperature, thermal reliability, and material compatibility. The present study demonstrates that $MgCl_2$–H_2O solutions possess several characteristics desirable for sub-zero latent heat thermal energy storage applications.

The observed phase transition temperatures are compatible with frozen-food preservation requirements, while the latent heat values indicate significant cold storage capacity. Furthermore, the macro-scale experiments confirm that thermal energy can be effectively stored and released under conditions representative of practical operation. These findings support previous studies that identified magnesium chloride hydrate systems as promising candidates for cold thermal energy storage applications [5, 6].

Nevertheless, the presence of supercooling and the corrosive nature of chloride-containing solutions remain important challenges that must be addressed before large-scale implementation. Future work should therefore focus on the incorporation of nucleating agents, thermal conductivity enhancement strategies, and corrosion mitigation approaches to improve overall system performance.

Considering the combined effects of latent heat capacity, phase transition temperature, supercooling behaviour, and material compatibility, the 21 wt.% $MgCl_2$ solution exhibited the most favourable overall performance. This concentration achieved the highest latent heat storage capacity while maintaining suitable low-temperature phase transition characteristics, making it the most promising candidate among the investigated formulations for sub-zero thermal energy storage applications.

5. Conclusions

All $MgCl_2$ solutions exhibited significant supercooling, with nucleation occurring near −45 °C and an average supercooling degree of approximately 10 °C. The 21 wt.% $MgCl_2$ solution exhibited the highest latent heat capacity of 171.34 J/g, indicating proximity to the eutectic composition. Increasing sample mass from 50 g to 500 g extended freezing and melting durations, demonstrating that macro-scale thermal behaviour cannot be predicted solely from DSC measurements. Corrosion testing revealed that stainless steel exhibited the highest resistance to chloride attack, while aluminium showed the greatest susceptibility to degradation. The combination of favourable phase change temperature (≈−34 °C), high latent heat capacity, and acceptable material compatibility suggests that the 21 wt.% $MgCl_2$ solution is the most suitable candidate for sub-zero thermal energy storage applications. Future work should explore long-term cycling and stabilisation strategies to address hydrate degradation and phase segregation in real-world deployments.

Acknowledgments

We would like to acknowledge the support and assistance provided by Tshwane University of Technology and University of South Africa staff members for the equipment and experimental setup. The authors acknowledge the use of AI tools Elicit Pro AI and Google Gemini Pro 3.1 for language editing. All edits were carefully reviewed and validated by the authors to ensure accuracy, compliance with academic standards, and research integrity. The authors fully support Academia.edu Journals' adherence to COPE guidelines on AI in publication ethics and confirm that this use has been managed responsibly and ethically.

Funding

This research received no external funding.

Author contributions

Conceptualization, T.B.R.; investigation, T.B.R., I.B.S. and J.M.M.; methodology, L.S. and L.R.K.; formal analysis, L.R.K.; resources, L.S., I.B.S. and J.M.M.; data curation, L.R.K., I.B.S. and J.M.M.; writing—original draft preparation, T.B.R.; writing—review and editing, A.U.C.N. and W.M.; validation, W.M.; supervision, Z.H.; project administration, Z.H. All authors have read and agreed to the published version of the manuscript.

Conflict of interest

The authors declare that they have no competing interests.

Data availability statement

All data supporting the findings of this publication are available within this article.

Publisher's note

Academia.edu Journals stays neutral regarding jurisdictional claims in published maps and institutional affiliations. All claims expressed in this article are solely those of the authors and do not necessarily represent those of their affiliated organizations, or those of the publisher, the editors, and the reviewers. Any product that may be evaluated in this article, or claim that may be made by its manufacturer, is not guaranteed or endorsed by the publisher.

Copyright

References

1. Rashid FL, Al-Obaidi MA, Dulaimi A, Bernardo LFA, Redha ZAA, Hoshi HA, et al. Recent advances on the applications of phase change materials in cold thermal energy storage: a critical review. J Compos Sci. 2023; 7 (8): 338. doi: 10.3390/jcs7080338
2. Rocha TTM, Teggar M, Trevizoli PV, de Oliveira RN. Potential of latent thermal energy storage for performance improvement in small-scale refrigeration units: a review. Renew Sustain Energy Rev. 2023; 187: 113746. doi: 10.1016/j.rser.2023.113746
3. Wang G, Tang Z, Gao Y, Liu P, Li Y, Li A, et al. Phase change thermal storage materials for interdisciplinary applications. Chem Rev. 2023; 123 (11): 6953–7024. doi: 10.1021/acs.chemrev.2c00572
4. Man X, Lu H, Xu Q, Wang C, Ling Z. Review on the thermal property enhancement of inorganic salt hydrate phase change materials. J Energy Storage. 2023; 72: 108699. doi: 10.1016/j.est.2023.108699
5. Jiang L, Lin YC, Liu W, Ma ZW, Wang RQ, Zhang XJ, et al. Thermophysical characterization of magnesium chloride and its application in open sorption thermal energy storage system. Sol Energy Mater Sol Cells. 2021; 232: 111528. doi: 10.1016/j.solmat.2021.111528

6. Yang X, Xie B, Li C, Xu L, Jin J, Qiu Y, et al. Emerging magnesium chloride hexahydrate phase change material targeting cold storage engineering. J Energy Storage. 2025; 137: 118639. doi: 10.1016/j.est.2025.118639
7. Tan S, Zhang X. Progress of research on phase change energy storage materials in their thermal conductivity. J Energy Storage. 2023; 61: 106772. doi: 10.1016/j.est.2023.106772
8. Wu T, Xie N, Niu J, Luo J, Gao X, Fang Y, et al. Preparation of a low-temperature nanofluid phase change material: $MgCl_2$–H_2O eutectic salt solution system with multi-walled carbon nanotubes (MWCNTs). Int J Refrig. 2020; 113: 136–44. doi: 10.1016/j.ijrefrig.2020.02.008
9. Balakrishnan VKV, Kumaresan K. System scale testing of magnesium chloride hexahydrate for thermal energy storage—a physical and numerical approach. J Taiwan Inst Chem Eng. 2023; 153: 104996. doi: 10.1016/j.jtice.2023.104996
10. Radebe TB, Ndanduleni AUC, Huan Z. Investigation of low-cost eutectic salts to ensure food products during power outages. J Energy Storage. 2023; 63: 106960. doi: 10.1016/j.est.2023.106960
11. Zhang S, Zhang S, Zeng J, Zhu F, Dang L, Sun S, et al. Phase change behavior and mechanical transformation of eutectic hydrated-salt phase-change gels tuned by water. ACS Appl Polym Mater. 2025; 7: 1540–8. doi: 10.1021/acsapm.4c03277
12. Höhlein S, König-Haagen A, Brüggemann D. Thermophysical characterization of $MgCl_2{\cdot}6H_2O$, xylitol and erythritol as phase change materials (PCM) for latent heat thermal energy storage (LHTES). Materials. 2017; 10 (4): 444. doi: 10.3390/ma10040444
13. Malaret F. Exact calculation of corrosion rates by the weight-loss method. Exp Results. 2022; 3: e9. doi: 10.1017/exp.2022.5
14. Ferrer G, Solé A, Barreneche C, Martorell I, Cabeza LF. Corrosion of metal containers for use in PCM energy storage. Renew Energy. 2015; 76: 465–9. doi: 10.1016/j.renene.2014.11.036
15. Xiao C, Zheng Y, Xu Z, Wang L. Influences of chloride on microstructure and corrosion behaviour of Al-Mg-Si alloys in neutral solution. Int J Electrochem Sci. 2022; 17: 22083. doi: 10.20964/2022.08.37
16. Krauß M, Herzog R, Scholtes B. Influence of surface treatment on the pitting corrosion behaviour of high alloyed stainless steels in a chloride solution. Int J Mater Res. 2001; 92 (8): 910–5. doi: 10.1515/ijmr-2001-0166
17. Zheng D, Wu X. Comprehensive evaluation of eutectic character used as low temperature thermal energy storage. Cryogenics. 2002; 1: 37–45.
18. Li G, Hwang Y, Radermacher R. Review of cold storage materials for air conditioning application. Int J Refrig. 2012; 35 (8): 2053–77. doi: 10.1016/j.ijrefrig.2012.06.003
19. Zhang X, Shi Q, Luo L, Fan Y, Wang Q, Jia G. Research progress on the phase change materials for cold thermal energy storage. Energies. 2021; 14 (24): 8233. doi: 10.3390/en14248233
20. Oró E, Miró L, Farid MM, Cabeza LF. Improving thermal performance of freezers using phase change materials. Int J Refrig. 2012; 35 (4): 984–91. doi: 10.1016/j.ijrefrig.2012.01.004
21. Zalba B, Marín JM, Cabeza LF, Mehling H. Review on thermal energy storage with phase change: materials, heat transfer analysis and applications. Appl Therm Eng. 2003; 23 (3): 251–83. doi: 10.1016/S1359-4311(02)00192-8
22. Wang Y, Sui J, Xu Z. Preparation and characterization of $CaCl_2{\cdot}6H_2O$ based binary inorganic eutectic system for low temperature thermal energy storage. Energy. 2022; 263: 125036. doi: 10.1016/j.energy.2022.125036